Modulating responses of toehold switches by an inhibitory hairpin

Soo-Jung Kim[+], Matthew Leong[+], Matthew B. Amrofell, Young Je Lee, and Tae Seok Moon*

Department of Energy, Environmental and Chemical Engineering, Washington University in St. Louis, St. Louis, MO, 63130, USA

[+] SJK and ML contributed equally to this work.

[*] To whom correspondence should be addressed.

Tae Seok Moon

One Brookings Dr., Box 1180

St. Louis, MO 63130, USA

Tel: +1 (314) 935-5026

Fax: +1 (314) 935-7211

Email: tsmoon@wustl.edu

Abstract

The toehold switch consists of a *cis*-repressing switch RNA hairpin and a *trans*-acting trigger RNA. The binding of the trigger RNA to an unpaired toehold sequence of the switch hairpin allows for a branch migration process, exposing the start codon and ribosome binding site for translation initiation. In this work, we demonstrate that responses of toehold switches can be modulated by introducing an inhibitory hairpin that shortens the unpaired toehold region length. First, we investigated the effect of the toehold region length on output gene expression, showing that the second trigger RNA, which binds to the inhibitory hairpin, is necessary for output gene activation when the hairpin-to-hairpin spacing is short. Second, the apparent Hill coefficient was found generally to increase with the decreasing hairpin-to-hairpin spacing or the increasing hairpin number. This work expands the utility of toehold switches by providing a new way to modulate their response.

Keywords

RNA regulator; toehold switch; AND gate; ultrasensitivity; hairpin structure

Impressive progress has been made in developing synthetic RNA regulators that control gene expression at the post-transcriptional or translational level[1-8]. Among them, the so-called toehold switches provide a wide dynamic range, which has been typically reached only by transcriptional regulators[4]. The utility of toehold switches has been demonstrated both in *E. coli* (by constructing ribocomputing systems[9]) and in cell-free systems (by developing low-cost virus detection kits[10, 11]). Modulating responses of toehold switches will expand their utility.

The toehold switch consists of both a *cis*-repressing switch RNA hairpin with an unpaired toehold sequence at the 5'-end and a *trans*-acting trigger RNA (Figure 1A). The switch RNA hairpin contains the start codon (AUG) and ribosome binding site (RBS), forming a bulge and a loop of the hairpin, respectively. The binding of a trigger RNA to the toehold sequence allows for a branch migration process, exposing AUG and RBS for translation initiation (as shown in Figures 1A and 1B using GFP as a reporter; for experiment detail, see the figure caption and Supplementary Methods).

Green et al. demonstrated that multiple switch RNA hairpins, each of which contains AUG and RBS, could be concatenated upstream of an output gene in the same reading frame to construct multi-input logic gates[9]. For example, when each hairpin contains AUG, RBS, and a sufficiently long unpaired toehold sequence at the 5'-end (~15 nt), a 2-input OR gate can be built using two trigger RNAs with different sequences, each of which binds to its corresponding unpaired toehold sequence. This excellent design enabled an impressive 12-input circuit to function robustly, while the output would be a mixture of reporter proteins with slightly different sizes due to additional amino acids incorporated into them for the upstream hairpin modules.

We started this study by asking the following question. What would be the effect of an RNA hairpin lacking AUG and RBS (G5 in Figure 1C), which is designed to shorten the unpaired toehold region length ('a' in Figure 1C) of the AUG/RBS-containing "primary" hairpin (G3n* in Figure 1C), on the response of the toehold switch? We hypothesized that the effect is inhibitory and instead of building an OR gate, we can modulate responses of toehold switches by changing the hairpin-to-hairpin spacing as well as the expression levels of the two trigger RNAs. While the inhibitory RNA hairpin lacks AUG and RBS, it contains an unpaired, full-length toehold sequence at the 5'-end to which its corresponding trigger RNA can bind. Thus, when the "secondary" trigger RNA (TrG5 in Figure 1C) binds to the inhibitory hairpin (G5 in Figure 1C), the unpaired, full-length toehold sequence ('*' + 'a' in Figure 1C) of the primary hairpin becomes exposed, facilitating its binding to the primary trigger RNA (TrG3n* in Figure 1C).

To test this idea, we built three different circuits (with 'a' length = 10, 7, or 4 nt; Figures 1C and 1D). The secondary trigger RNA (TrG5) was transcribed by the 3OC6-inducible promoter (pLux; 3OC6, 3-oxohexanoyl-homoserine lactone), and the primary trigger RNA (TrG3n* where * is 5, 8, or 11) was transcribed by the IPTG-inducible promoter (pLac; IPTG, isopropyl β-D-1-thiogalactopyranoside). The switch RNA (Sw-G5-G3n* where * is 5, 8, or 11) was expressed by a constitutive promoter (http://parts.igem.org/Part:Bba_J23104). When the spacing is sufficiently long (10 nt), TrG3n5 would have a high chance of base-pairing with Sw-G5-G3n5 even in the absence of TrG5 (as shown in the upper route in Figure 1C), making the circuit behave like a one-input switch with a secondary tuning knob for the other input. In this circuit, TrG3n5 (IPTG) acts as its primary input molecule, while TrG5 (3OC6) acts as an auxiliary input molecule for output

range tuning. In contrast, TrG3n11 (a=4) would need TrG5-hairpin binding to expose the unpaired, full-length toehold sequence of the primary hairpin (the lower route in Figure 1C), making the circuit behave like a 2-input AND gate. When tested at a combination of different IPTG (0-10 mM) and 3OC6 (0-5 μM) concentrations, the circuits showed the expected responses (Figure 1D).

Ultrasensitivity is an important property of a genetic circuit that allows for filtering small, temporary stimuli in fluctuating environments. Ultrasensitive responses can be generated by a variety of mechanisms, among which cooperativity is prevalent in genetic circuits[12, 13]. Intrigued by the result that both trigger RNAs were required for maximum output gene expression (the lower route in Figure 1C for a=4), we hypothesized that ultrasensitivity can be observed when one trigger RNA binds to both hairpins. To test this idea, we constructed a two-hairpin switch RNA (Sw-T0-T3) that is composed of two hairpin modules containing the same trigger RNA binding sequence (Figure 2A). As a control switch, a toehold switch with one hairpin (Sw-T3) was also built. When tested, the toehold switch with two hairpins showed an apparent Hill coefficient of 7.0, while the toehold switch with one hairpin showed an apparent Hill coefficient of 2.8 (Figure 2B).

To further study ultrasensitive responses of toehold switches with multiple trigger RNA binding sites, we designed and constructed two new sets of toehold switches. First, to investigate the effect of the hairpin-to-hairpin spacing on the apparent Hill coefficient, twelve toehold switches containing two trigger RNA binding sites were built and tested. As shown in Figure 2C, the apparent Hill coefficient generally increased with the decreasing hairpin-to-hairpin spacing (R^2 = 0.52). Consistent with the trend shown in Figure 1D, this result implies that the short spacing may facilitate cooperative binding of the trigger RNA by reducing its accessibility (i.e., binding

probability) to the primary hairpin and by promoting its sequential binding (i.e., binding to the inhibitory hairpin prior to the primary one). However, the apparent Hill coefficient also varied within the switch group of the same spacing. Investigating the effect of the other factors systematically (e.g., the size of hairpin loops and stems and the Gibbs free energy change involved in the complex, multiple intra- and intermolecular RNA-RNA interactions) on ultrasensitive responses of toehold switches would be a potential future study. Second, we tested ultrasensitivity behaviors of toehold switches containing up to three trigger RNA binding sites. As shown in Figure 2D, the apparent Hill coefficient (n_H) was found to increase with the increasing number of trigger RNA binding sites. It is worth noting that these three toehold switch RNA sequences (Figure 2D) were designed differently from that of Sw-T0-T3 and Sw-T3 (Figure 2B) to demonstrate that the trend (n_H vs the binding site number) was observed from at least two different sets of toehold switches. Together, we showed that responses of toehold switches can be modulated by introducing an inhibitory hairpin, and this strategy can be a generalizable principle.

It is worth noting that our toehold switch showed a relatively low dynamic range (e.g., ~20X in Figure 1B which is lower by one order of magnitude, compared to that of the best switch from Green et al.[4]). This is due to the differences in RNA sequences, strains, reporters, expression systems, plasmid copy numbers, and importantly, the choice of OFF strains (i.e., no cognate input RNA expressed vs. input RNA expressed at the basal level due to the leaky input promoter)[4, 9]. Indeed, when calculated using the strain containing only the pG3n5 plasmid as the OFF strain (Supplementary Figure S7), the dynamic range was up to ~270X (i.e., no input RNA expressed), instead of ~20X (i.e., input RNA expressed at the basal level), showing the effect of the leaky input promoter (Supplementary Figure S3) on the dynamic range.

Recently, regulatory RNAs have attracted researchers' attention due to their advantages over protein regulators as previously discussed[14]. Among those advantages, relatively simple structures and straightforward base pairing rules make the *de novo* design of RNA regulators simpler than that of protein regulators by using computational tools[15, 16]. However, rational creation of new RNA regulators, which rely on novel modes of molecular interaction, is still a challenging task[4, 17-19]. Alternatively, previously developed interaction modes can be modified to implement tunable and sophisticated control of gene expression. In this work, we demonstrated a novel way to modulate responses of toehold switches by rationally modifying them. By introducing an inhibitory hairpin that was rationally designed using computational tools[15, 16], we were able to build a genetic circuit with dual knobs for output fine-tuning, a 2-input AND gate, and multiple tunable ultrasensitive switches. The strategy developed herein sets a foundation for more sophisticated control of gene expression by toehold switches.

SUPPORTING INFORMATION

Supplementary Methods, Supplementary Figures S1-S7, and Supplementary Tables S1-S2 are available.

AUTHOR CONTRIBUTIONS

SJK, ML, MBA, and YJL performed experiments. SJK, ML, MBA, and TSM analyzed results and wrote the manuscript.

ACKNOWLEDGEMENT

This work was supported by the National Science Foundation (MCB-1714352 and CBET-1350498).

CONFLICT OF INTEREST

The authors declare no conflict of interest.

References

[1] Lee, Y. J., and Moon, T. S. (2018) Design rules of synthetic non-coding RNAs in bacteria, *Methods 143*, 58-69.

[2] Hoynes-O'Connor, A., and Moon, T. S. (2016) Development of Design Rules for Reliable Antisense RNA Behavior in E. coli, *ACS Synthetic Biology 5*, 1441-1454.

[3] Na, D., Yoo, S. M., Chung, H., Park, H., Park, J. H., and Lee, S. Y. (2013) Metabolic engineering of *Escherichia coli* using synthetic small regulatory RNAs, *Nat Biotechnol 31*, 170-174.

[4] Green, A. A., Silver, P. A., Collins, J. J., and Yin, P. (2014) Toehold switches: de-novo-designed regulators of gene expression, *Cell 159*, 925-939.

[5] Winkler, W., Nahvi, A., and Breaker, R. R. (2002) Thiamine derivatives bind messenger RNAs directly to regulate bacterial gene expression, *Nature 419*, 952-956.

[6] Jang, S., Jang, S., Yang, J., Seo, S. W., and Jung, G. Y. (2018) RNA-based dynamic genetic controllers: development strategies and applications, *Current opinion in biotechnology 53*, 1-11.

[7] Carothers, J. M., Goler, J. A., Juminaga, D., and Keasling, J. D. (2011) Model-driven engineering of RNA devices to quantitatively program gene expression, *Science (New York, N.Y 334*, 1716-1719.

[8] Win, M. N., and Smolke, C. D. (2007) A modular and extensible RNA-based gene-regulatory platform for engineering cellular function, *Proc Natl Acad Sci U S A 104*, 14283-14288.

[9] Green, A. A., Kim, J., Ma, D., Silver, P. A., Collins, J. J., and Yin, P. (2017) Complex cellular logic computation using ribocomputing devices, *Nature 548*, 117-121.

[10] Pardee, K., Green, A. A., Ferrante, T., Cameron, D. E., DaleyKeyser, A., Yin, P., and Collins, J. J. (2014) Paper-based synthetic gene networks, *Cell 159*, 940-954.

[11] Pardee, K., Green, A. A., Takahashi, M. K., Braff, D., Lambert, G., Lee, J. W., Ferrante, T., Ma, D., Donghia, N., and Fan, M. (2016) Rapid, low-cost detection of Zika virus using programmable biomolecular components, *Cell 165*, 1255-1266.

[12] Ferrell, J. E., and Ha, S. H. (2014) Ultrasensitivity part III: cascades, bistable switches, and oscillators, *Trends Biochem Sci 39*, 612-618.

[13] Shopera, T., Henson, W. R., Ng, A., Lee, Y. J., Ng, K., and Moon, T. S. (2015) Robust, tunable genetic memory from protein sequestration combined with positive feedback, *Nucleic Acids Res 43*, 9086-9094.

[14] Lee, Y. J., Hoynes-O'Connor, A., Leong, M. C., and Moon, T. S. (2016) Programmable control of bacterial gene expression with the combined CRISPR and antisense RNA system,

Nucleic Acids Res 44, 2462-2473.
[15] Zuker, M. (2003) Mfold web server for nucleic acid folding and hybridization prediction, *Nucleic Acids Res 31*, 3406-3415.
[16] Zadeh, J. N., Steenberg, C. D., Bois, J. S., Wolfe, B. R., Pierce, M. B., Khan, A. R., Dirks, R. M., and Pierce, N. A. (2011) NUPACK: Analysis and design of nucleic acid systems, *J Comput Chem 32*, 170-173.
[17] Lee, Y. J., Kim, S. J., and Moon, T. S. (2018) Multilevel regulation of bacterial gene expression with the combined STAR and antisense RNA system, *ACS Synth Biol 7*, 853-865.
[18] Chappell, J., Takahashi, M. K., and Lucks, J. B. (2015) Creating small transcription activating RNAs, *Nat Chem Biol 11*, 214-U165.
[19] Qi, L. S., Larson, M. H., Gilbert, L. A., Doudna, J. A., Weissman, J. S., Arkin, A. P., and Lim, W. A. (2013) Repurposing CRISPR as an RNA-guided platform for sequence-specific control of gene expression, *Cell 152*, 1173-1183.

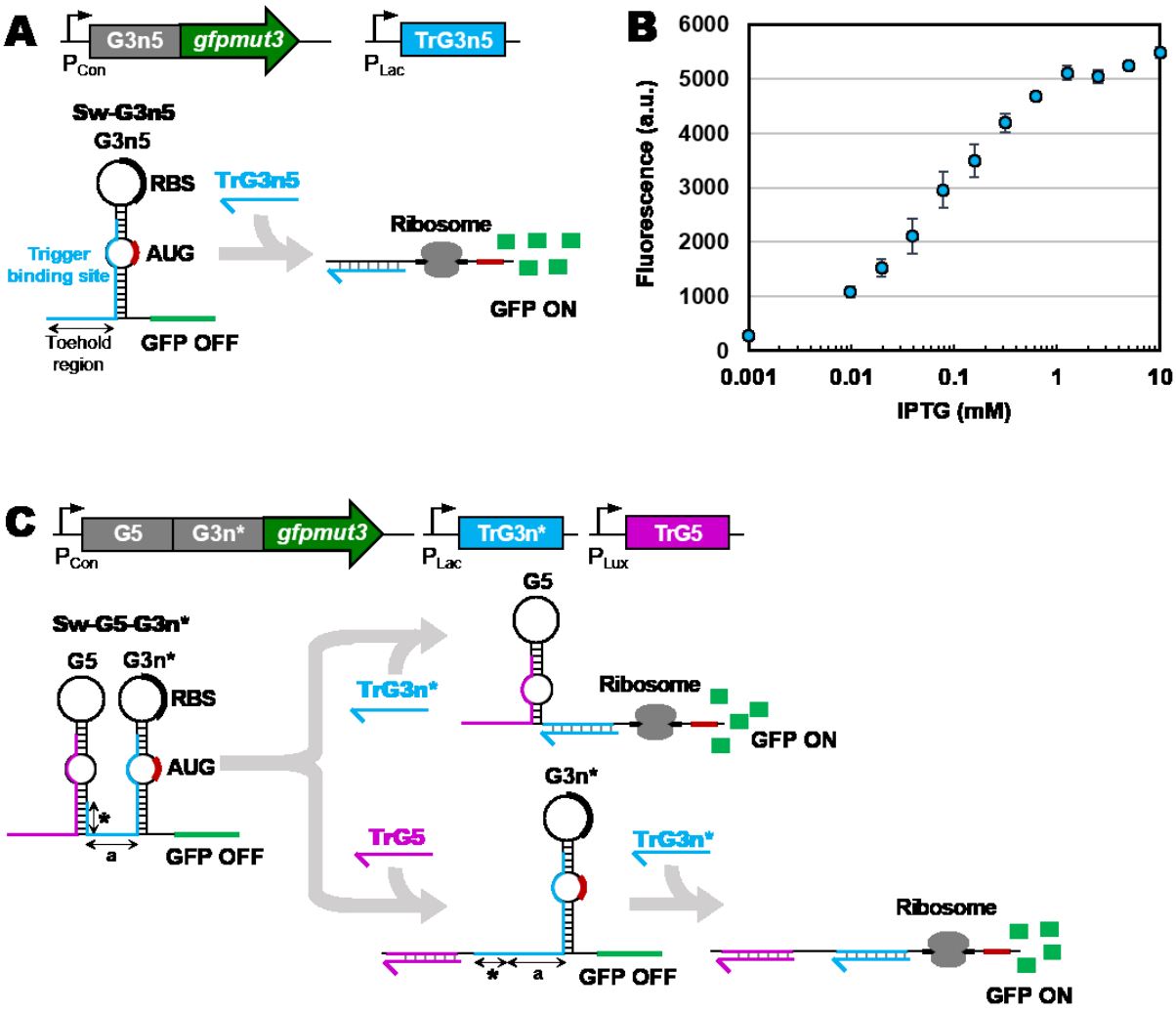

Switch RNA	Sw-G5-G3n5	Sw-G5-G3n8	Sw-G5-G3n11
' * ' length (nt)	5	8	11
' a ' length (nt)	10	7	4
Trigger RNA	TrG5 / TrG3n5	TrG5 / TrG3n8	TrG5 / TrG3n11

Figure 1. A two-hairpin switch RNA and two-trigger RNA system in DH10B strains. (A) Schematic diagram of the one-hairpin switch RNA and one-trigger RNA system (see

Supplementary Figure S1 and Table S2 for detail). The switch RNA (Sw-G3n5) expressed by a constitutive promoter (Bba_J23104) contains a hairpin module (G3n5) with ribosome binding site (RBS; bold and black) and start codon (red) upstream of the *gfpmut3* gene (green). The toehold domain was restricted to 15 nucleotides at the 5'-end of the hairpin structure. The sequestration of RBS and start codon in the hairpin structure blocks GFP translation. The trigger RNA (TrG3n5; sky blue) transcribed by the IPTG-inducible promoter (pLac) binds to its complementary sequence (also shown in sky blue) in the Sw-G3n5. Consequently, the hairpin structure is disrupted, and the RBS and start codon are exposed, leading to initiation of GFP translation. **(B)** Activation of GFP expression by varying the trigger RNA expression level in the one-hairpin switch RNA (Sw-G3n5) and one-trigger RNA (TrG3n5) system (in the DH10B strain). The experiment was performed at IPTG concentrations of 0, 0.01, 0.02, 0.04, 0.08, 0.16, 0.31, 0.63, 1.25, 2.5, 5 and 10 mM. The fluorescence (a.u.) is reported by calculating $[(F_{experimental}/Abs_{experimental}) - (F_{negative\ control}/Abs_{negative\ control})]$, where the negative control is the DH10B strain without a plasmid. F is the measured fluorescence (excitation at 483 nm and emission at 530 nm), and Abs is the measured absorbance at 600 nm. The error bars represent the standard deviation of the fluorescence values from three biological replicates. **(C)** Schematic diagram of the two-hairpin switch RNA and two-trigger RNA system (see Supplementary Figure S1 and Table S2 for detail). The two-hairpin switch RNA (Sw-G5-G3n*) is composed of a hairpin module with an RBS sequence and start codon (G3n*) and an additional hairpin module without both parts (G5). The Sw-G5-G3n* is designed for its trigger RNAs (TrG5 and TrG3n*) to bind to G5 and G3n*, respectively, where '*' denotes the number of nucleotides in the G5 stem to which TrG3n* is complementary. The TrG3n* binds to its complementary sequence and initiates GFP translation. Additional trigger RNA (TrG5) transcribed by the 3OC6-inducible promoter (pLux) binds to the G5 hairpin. The 'a' + '*' length is 15 nt, where 'a' denotes the 'unpaired' spacing between the two hairpins. **(D)** Dependence of circuit outputs on the 'a' length in the two-hairpin switch RNA (Sw-G5-G3n*) and two-trigger RNA (TrG5 and TrG3n*) system (in the DH10B strain). With a sufficiently long hairpin-to-hairpin spacing (a=10), TrG3n5 would have a high chance of intermolecular base-pairing with mRNA (even in the absence of TrG5, as shown in the upper route in 1C), while TrG3n11 (a=4) would need TrG5-hairpin base-pairing first to expose its complementary sequence that is long enough for TrG3n11-hairpin binding (the lower route in 1C). In other words, the role of TrG5 varies from an auxiliary input molecule of the one-input switch, where TrG5 can modulate just output ranges (a=10), to a primary input molecule of the two-input AND gate (a=4). Relative expression level is calculated by dividing the fluorescence values ($[(F_{experimental}/Abs_{experimental}) - (F_{negative\ control}/Abs_{negative\ control})]$) by the maximum fluorescence value from each system (see Supplementary Figure S2 for the data without normalization by the maximum value). The experiments were performed at IPTG concentrations of 0, 0.01, 0.02, 0.04, 0.08, 0.16, 0.31, 0.63, 1.25, 2.5, 5 and 10 mM (from left to right) to transcribe TrG3n5, TrG3n8 or TrG3n11; and 3OC6 concentrations of 0, 0.005, 0.01, 0.025, 0.05, 0.25, 1 and 5 μM (from bottom to top) to transcribe TrG5. Experimental data are the average of three biological replicates.

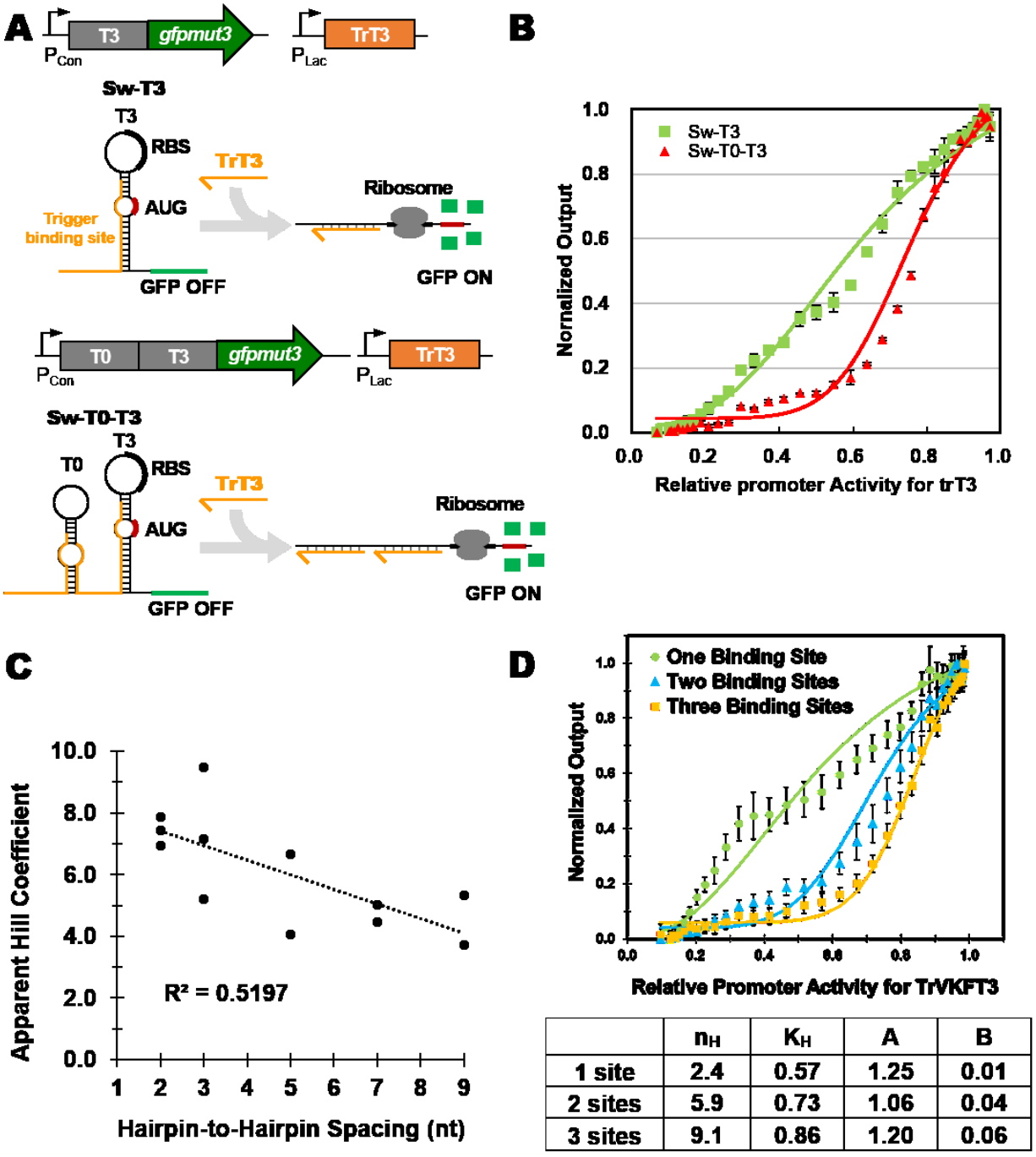

	n_H	K_H	A	B
1 site	2.4	0.57	1.25	0.01
2 sites	5.9	0.73	1.06	0.04
3 sites	9.1	0.86	1.20	0.06

Figure 2. A two-hairpin switch RNA and one-trigger RNA system. (A) Schematic diagram of the two-hairpin switch RNA and one-trigger RNA system (see Supplementary Figure S1 and Table S2 for detail). The two-hairpin switch RNA (Sw-T0-T3) is composed of two hairpin modules. The first hairpin (T3) consists of an RBS and start codon, and the second hairpin (T0) without both parts is placed upstream of T3. The TrT3 trigger RNA (orange) is designed to bind to two different sites in the T0 and T3 hairpins. The Sw-T0-T3 and TrT3 were expressed using a constitutive promoter (Bba_J23104) and an inducible promoter (pLac), respectively. The one-hairpin switch RNA (Sw-T3) and one-trigger RNA (TrT3) system is also shown as the control circuit. **(B)**

Ultrasensitivity behavior observed with the two-hairpin switch RNA (Sw-T0-T3) and one-trigger RNA (TrT3) system (in the DH10B strain). The experiment was performed at 36 different IPTG concentrations (0–20 mM), and the following equation was used to obtain fluorescence outputs: $F_{out} = [(F_{experimental}/Abs_{experimental}) - (F_{negative\ control}/Abs_{negative\ control})]$, where the negative control is the DH10B strain without a plasmid. F is the measured fluorescence (excitation at 483 nm and emission at 530 nm), and Abs is the measured absorbance at 600 nm. Data were fit to the Hill-type equation (Supplementary Methods for detail) and R^2 values were greater than 0.95: $A[P_x^{n_H} / (P_x^{n_H} + K_H^{n_H})] + B$, where P_x is the relative promoter activity for TrT3 (Supplementary Figure S3). The apparent Hill coefficients (n_H) of one-hairpin switch RNA (Sw-T3) and two-hairpin switch RNA (Sw-T0-T3) are 2.8 (with $K_H = 0.64$, $A = 1.20$, and $B = 0.02$) and 7.0 (with $K_H = 0.76$, $A = 1.10$, and $B = 0.04$), respectively. The normalized output $((F_{out} - F_{min})/(F_{max} - F_{min}))$ is shown here (where F_{min} and F_{max} are the minimum and maximum fluorescence outputs, respectively), and the data without normalization are shown in Supplementary Figure S4. The error bars represent the standard deviation of the normalized values from three biological replicates. **(C)** The apparent Hill coefficient generally increased with the decreasing hairpin-to-hairpin spacing (in the BL21 Star (DE3) strains; see Supplementary Figure S5 for the corresponding data). **(D)** Ultrasensitivity behaviors were also observed with toehold switches containing three trigger RNA binding sites in the BL21 Star (DE3) strain. Similarly to 2A-2B, the switch RNA and the trigger RNA (TrVKFT3) were expressed using a constitutive promoter (Bba_J23104) and an inducible promoter (pLac), respectively, but the switch RNA sequences were designed differently from that of Sw-T0-T3 and Sw-T3 with up to three trigger RNA binding sites. The experiment was performed at 36 different IPTG concentrations (0–40 mM). Data were fit to the Hill-type equation (Supplementary Methods for detail) and R^2 values were greater than 0.95. The data without normalization are shown in Supplementary Figure S6. The error bars represent the standard deviation of the normalized values from six biological replicates.

Graphical Table of Contents